http://dx.doi.org/10.4322/tmm.2012.019

POWDER INJECTION MOLDING OF SIC FOR THERMAL MANAGEMENT

Valmikanathan Onbattuvelli [1]
Sachin Laddha [2]
Seong-Jin Park [3]
Jupiter Palagi de Souza [4]
Sundar Vedanarayan Atre [5]

Abstract

Silicon carbide (SiC) exhibits many functional properties that are relevant to applications in electronics, aerospace, defense and automotive industries. However, the successful translation of these properties into final applications lies in the net-shaping of ceramics into fully dense microstructures. Increasing the packing density of the starting powders is one effective route to achieve high sintered density and dimensional precision. The present paper presents an in-depth study on the effects of nanoparticle addition on the powder injection molding process (PIM) of SiC powder-polymer mixtures. In particular, bimodal mixtures of nanoscale and sub-micrometer particles are found to have significantly increased powder packing characteristics (solids loading) in the powder-polymer mixtures. The influence of nanoparticle addition on the multi-step PIM process is examined. The above results provide new perspectives which could impact a wide range of materials, powder processing techniques and applications.
Key words: Powder injection molding; Nanoparticles; Thermal management; SiC.

1 INTRODUCTION

Silicon carbide (SiC) has a useful combination of properties including high thermal conductivity, low coefficient of thermal expansion, mechanical strength and chemical inertness. In order to translate these properties into demanding applications in electronic, energy and transportation sectors, it is necessary to develop net-shaping processes that result in fully dense microstructures.[1] Among net-shaping techniques, powder injection molding (PIM) is considered to be well-suited for mass production of dimensionally precise, complex part geometries from metals or ceramics (Figure 1). Ceramic or metal powder is compounded with polymers and used to mold parts in an injection molding machine, in a manner analogous to the forming of conventional thermoplastics.[2] The molded part is then subjected to polymer removal (debinding). The debound part is then sintered under controlled time, temperature and atmospheric conditions to get the final part of desired dimensions, density, microstructure and properties. However, the successful application of PIM to SiC faces many hurdles. Firstly, defects are possible in the injection-molded components. During debinding, the goal is to remove the polymers in the shortest time with the least impact on the molded part. Additionally, SiC cannot be sintered easily due to covalent bonding. Additives are used in such systems to drive the densification by forming a liquid phase. The present paper examines the consequences of nanoparticle addition on the structure, processing and properties of SiC by PIM.

2 MATERIALS AND METHODOLOGY

The starting powder materials contained as-received, commercially available SiC with AlN and Y_2O_3 as the sintering additives. A multi-component polymer system based on paraffin wax, polypropylene was chosen as the binder to facilitate a multi-step debinding process. Torque rheometry was performed

[1]*PhD Student, School of Mechanical, Industrial, and Manufacturing Engineering – MIME, Oregon State University – OSU, 97331, Corvallis, OR, United States of America. E-mail: valmikanathan@gmail.com*
[2]*Research Engineer, Materials Division, Pacific Northwest National Laboratory – PNNL, 99354, Richland, WA, United States of America. E-mail:sgladdha@gmail.com*
[3]*Mechanical Engineering, Associate Professor, Pohang University of Science & Technology – POSTECH, Pohang, 790-784, Gyungbuk, Republic of Korea. E-mail: sjpark87@postech.ac.kr*
[4]*Materials, Professor, Universidade Federal Rio Grande do Sul – UFRGS, Av. Paula Gama, 110, Cep 90040-060, Porto Alegre, RS, Brasil. E-mail: jps@ufrgs.bre*
[5]*Associate Professor, Oregon Nanoscience & Microtechnologies Institute – ONAMI, School of Mechanical, Industrial, and Manufacturing Engineering – MIME, 97331, Corvallis, OR, USA. E-mail: sundar.atre@gmail.com*

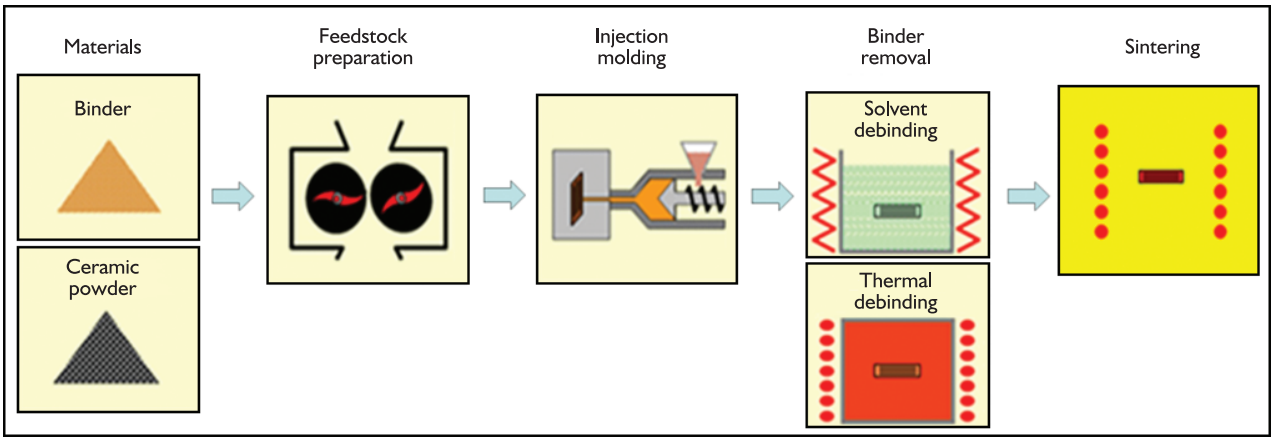

Figure 1. Overview of PIM, showing the flow from powders to the sintered part.

in the Intelli-Torque Plasticorder (Brabender) in order to determine the maximum packing density of the powder-polymer mixture. Twin screw extrusion of SiC feedstocks was performed with an Entek co-rotating 27 mm twin screw extruder with an L/D ratio of 40 and pelletized for further use. Moldflow software was used for simulating the injection conditions. Injection molding was performed on an Arburg 221M injection molding machine. Thermogravimetric analysis (TGA) was performed on the extruded feedstocks using TA-Q500 (TA instruments) thermal system operated under nitrogen flow in the temperature range of 50-600°C with a heating rate of 20°C/min. The rheological characteristics of the feedstock were examined on a Gottfert Rheograph 2003 capillary rheometer at different shear rates and temperatures. The testing was carried out in accordance with ASTM D 3835. Powder injection molded bimodal μ-n SiC samples were solvent and thermally debound prior to sintering. Heptane (Fischer Scientific) was used as the solvent to dissolve the soluble binder components at 40°C. Thermal debinding cycles of the solvent debound samples were performed under inert atmosphere in the CM 1212 FL furnace. Thermally debound bimodal SiC samples with an initial density of 2.15 g/cc (65% relative density) were pressureless sintered at different temperatures up to 1900°C for 4 hours under nitrogen atmosphere. The micrographs of the thermally debound and sintered samples were taken with the QuantaTM–FEG (FEI) dual beam scanning electron microscope (SEM) coupled with an energy dispersive X-ray spectrometer (EDAX). The density for all the sintered samples was measured with a lab-built Archimedes apparatus. The thermal diffusivity of the samples was measured with a LFA-457 (Netzsch) laser flash apparatus. TA Instruments- Q-500 was used to measure the specific heat (C_p) of the sintered samples. Vickers hardness and indentation toughness were measured using a Leco microhardness tester.

3 RESULTS AND DISCUSSION

SEM was performed on the monomodal and bimodal samples to examine the increase in the powder content with the nanoparticle addition for the SiC system (Figure 2). It can be noticed that in the bimodal powder--polymer mixtures, the nanoparticles fit into the interstitial spaces between the microparticles for the SiC system.

The mixing torque is plotted as a function of solids loading in Figure 3 for the monomodal and bimodal SiC systems. From the figure, it can be noticed mixing torque increases as a function of solids loading for both material systems. In addition, the mixing torque was found to generally decrease by the addition of nanoparticles. This behavior can be attributed to a lower suspension viscosity in bimodal mixtures, possibly due to the higher packing capability observed in the bimodal mixtures leading to lesser hydrodynamic friction between the powder and polymer phases. a maximum powder content of 87 wt.% (65 vol.%) in the powder-polymer mixture was achieved for the bimodal SiC mixture 90 wt.% μ- SiC and 10 wt.% n-SiC.

Comparative experiments for monomodal 100 wt.% μ-SiC systems, resulted in a maximum powder content of only 81 wt.% (53 vol.%) in the powder-polymer mixture. Further, the monomodal 100 wt.% n-SiC system showed a maximum powder content below 75 wt.%. Thus, a synergistically improved packing tendency can be observed for the mixtures of microscale and nanoscale powders. From the above findings, formulations with optimal solids loading (ϕ) of 58 and 51 vol.% for bimodal and monomodal SiC respectively, were compounded using twin screw extrusion.

Nanoparticles are well known to exhibit poor packing density owing to their tendency to agglomerate. Hence, the current finding of using nanoparticles to increase the solids loading appears to be rather interesting. However, the successful processing of these bimodal mixtures (with higher powder content) is contingent upon

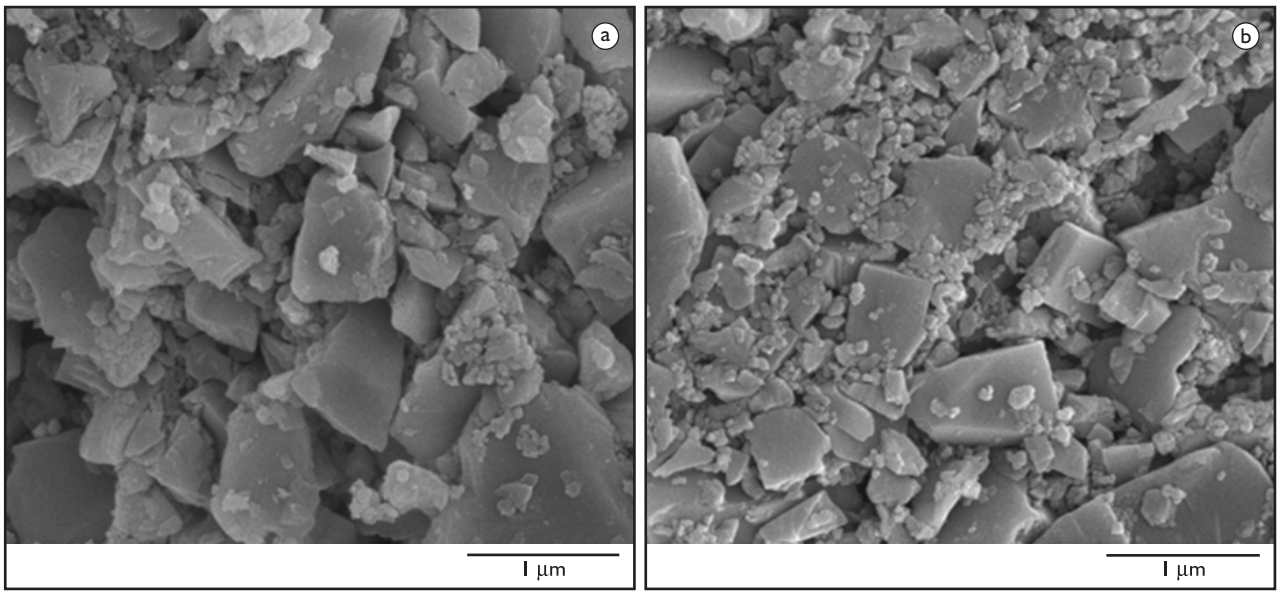

Figure 2. Powder packing behavior of monomodal (a) and bimodal (b) SiC powder-polymer mixtures.

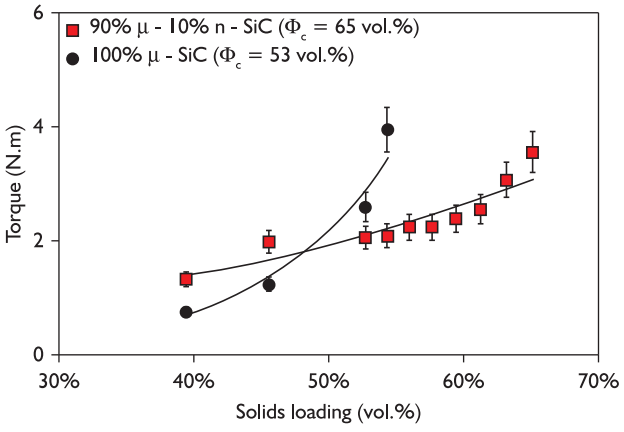

Figure 3. Mixing torque behavior of monomodal and bimodal SiC powder-polymer mixtures.

an in-depth understanding of the rheological behavior of such mixtures. Thus, the apparent viscosity-shear rate curves of SiC powder-polymer mixtures were measured at different temperatures, as shown in the Figure 4. The viscosity of the SiC bimodal powder-polymer mixture is found to be higher that of the monomodal powder--polymer mixtures at any given shear rate - temperature conditions.[3] This could be due to the increased solids loading as well as the presence of nanoparticles in the mixtures. Irrespective of the powder composition, the viscosity of all the powder-polymer mixtures decreased with an increase in shear rate, indicating pseudoplastic behavior. This is confirmed by evaluating the slope of such viscosity plots which represent (n-1), where "n" is the power law coefficient. The plots in our current case hold a negative slope with value of (1-n) as 0.84 and 0.93 for the monomodal and bimodal systems, respectively.

An attempt was made to analytically separate the contributions of reduced particle size from the increased solids loading by computing viscosity values at comparable solids loadings. A number of theoretical as well as empirical equations have been developed to predict the rheological behavior of suspensions. However, several of these equations are derived for dilute suspensions of spheres in Newtonian liquids. For the current study, it is necessary to consider models that take into account the maximum powder content ϕ_c, for predicting the viscosity of concentrated suspensions. For our current work on powder-polymer mixtures with higher powder content, the simplified Krieger-Dougherty model is utilized for a detailed comparison of the mixture rheology (Equation 1), where ϕ is the actual solids loading, ϕ_c is the critical solids loading, and η is the viscosity of the binder or powder--polymer mixture, depending on the subscript:

$$\eta_{mixture} = \frac{\eta_{binder}}{\left[1 - \frac{\phi}{\phi_c}\right]^2} \quad (1)$$

Equation 1 is used to compute the mixture viscosity, for various volumetric fractions of powder-polymer mixutres with the experimental values of ϕ_c. The trends are compared in Figure 5 at shear rates of 400 and 800 s^{-1} for a melt temperature of 160°C. From the analysis, it can be seen that the bimodal powder-polymer mixtures tend to show more fluidity than the monomodal systems. The lower viscosity in bimodal mixtures can be attributed to the effect of better powder packing and reduced critical solids loading. Similar trend computations are reported in the past where the shear viscosity of glass-beads (of various sizes) suspended in mineral oil was investigated.[4]

A series of injection molding runs were performed with the monomodal and bimodal SiC feedstocks to mold a multi-slotted part as shown in the Figure 6. Additionally, thermal and rheological properties were measured on the feedstocks and mold-filling simulations were performed using the Moldflow software. Figure 6 also depicts the progressive filling pattern during injection molding of SiC feedstocks.

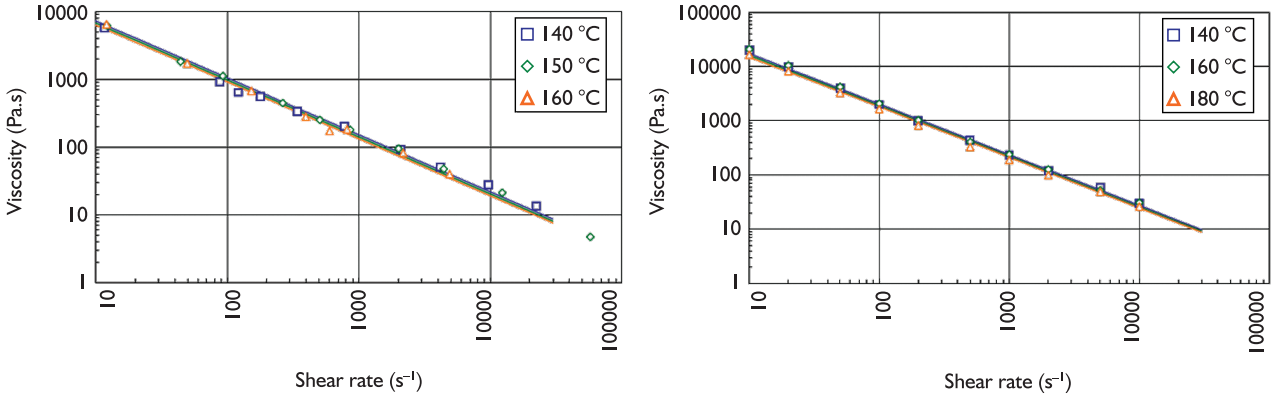

Figure 4. Rheological behavior of monomodal (left) and bimodal (right) SiC powder-polymer mixtures.

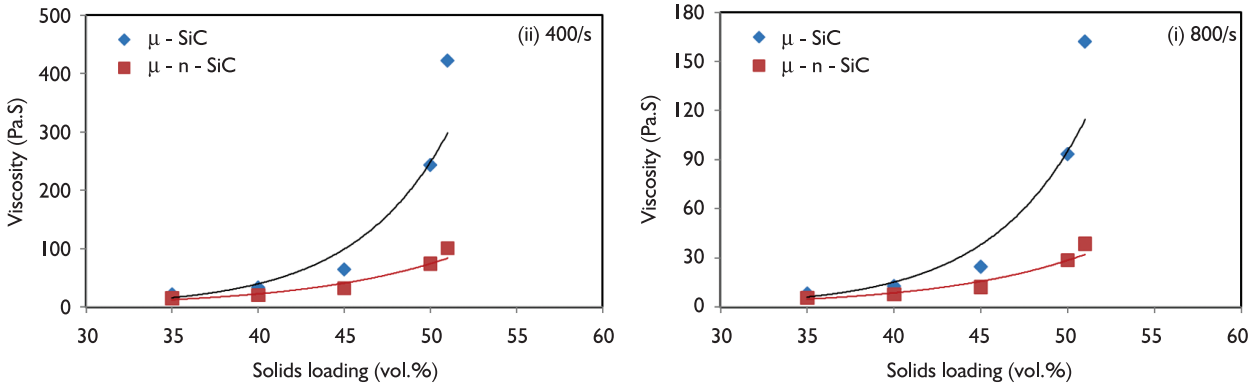

Figure 5. Separating the influence of nanoparticle additions and solids loading in SiC powder-polymer mixtures using the simplified Krieger-Dougherty equation.

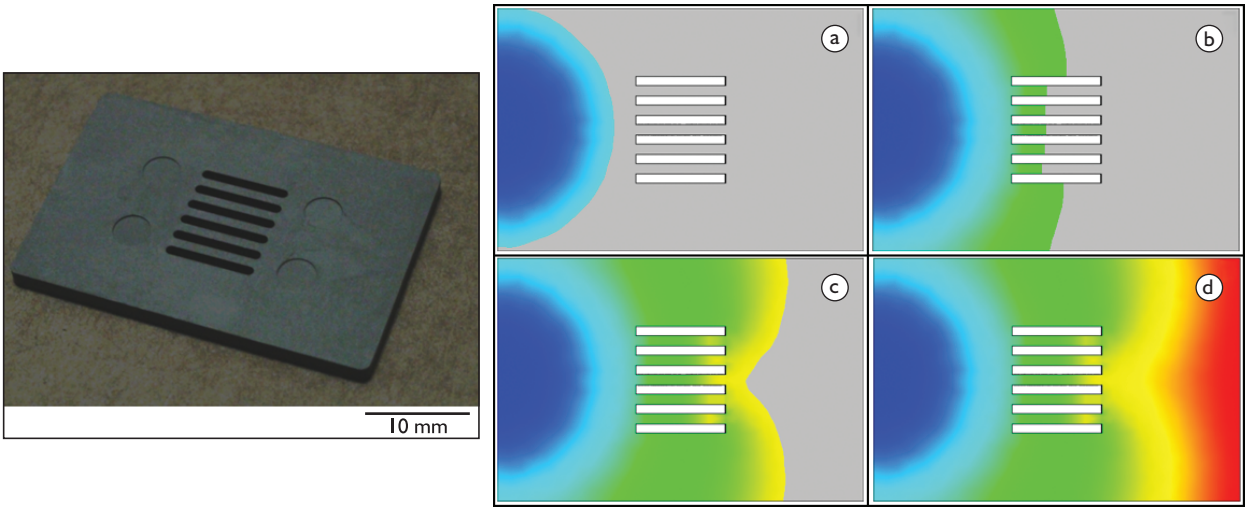

Figure 6. Progressive filling pattern during the injection molding of SiC feedstock at 170°C, (a) 25% fill, (b) 50% fill, (c): 75% fill and (d) 100% fill. The molded part is shown at the left for reference.

Simulations were performed to evaluate the effects of melt temperatures and feedstock viscosity on the mold filling behavior. Thus, an average melt velocity is calculated and plotted against melt temperature (Figure 7a). The lower melt velocity values can be explained by the reduced fluidity of the bimodal feedstocks due to a higher solids loading. These reduced velocity values can be directly correlated to the increased mold filling time, leading to heat transfer through the mold wall, resulting in the formation of a thick frozen layer narrowing the actual flow channel. This resulted in the increased shear stress at the walls for the bimodal feedstocks as plotted in the Figure 7b.

The reduced particle size and increased solids loading in bimodal SiC systems corresponds to reduced pore size and porosity. This in turn will increase the tortuous path, slowing the rate of binder removal from the injection molded parts.[5,6] Therefore, the effect of nanoparticle addition on the solvent debinding kinetics of injection molded SiC samples was studied. Figure 8 shows SEM micrographs of monomodal and bimodal SiC samples following different solvent debinding times, at 40°C. The surface micrograph of the region close to specimen surface after initial immersion in heptane show porous structure due to the elimination of soluble components, while no appreciable changes are observed in the micrograph of the specimen. By increasing the immersion time, the specimen microstructures at areas near the core and the surface become similar, indicates the removal of soluble components.

Figure 9 shows the soluble binder remaining (%) in heptane at different times for samples with various surface area-to-volume ratios from monomodal and bimodal SiC samples. Increasing the solvent immersion time and the surface area-to-volume ratio decreased the residual soluble binder, at any given temperature. Further, the monomodal samples show shorter solvent debinding times as a result of the lower solids loading and possibly higher particle size.

Following solvent debinding, the SiC samples were subject to thermal debinding. In order to follow the pyrolysis behavior during thermal debinding, TGA runs were performed. From the TGA plots (Figure 10), the powder content in the SiC monomodal and bimodal feedstocks was determined to be 79.5 ± 0.2 wt.% and 82 ± 0.2 wt.%, respectively. The two stage degradation exhibited by the feedstocks corresponds to the degradation of the filler phase from 175-400°C and backbone polymers from 400-550°C. Figures 10 also reveals a shift in the degradation peaks for the SiC bimodal feedstocks. This expedited degradation can be tentatively attributed to the catalytic effect of nanoparticles. However, further research is required in studying the effect of nanoparticle addition on the residual carbon during the thermal debinding stage.

Following debinding, sintering runs were conducted for the SiC samples. From Figure 11a, it can be seen that the densification of the bimodal μ-n SiC was initiated at or below 1550°C. This onset temperature is at least 100°C lower than most prior reports in the literature.[7-12] SEM studies on these samples showed the liquid phase formation at ~1550°C (Figure 12). Additionally, a novel nanorod formation was observed for the monomodal μ-SiC samples that was absent in the bimodal μ-n SiC samples. A shift in the densification towards lower sintering temperatures can be correspondingly expected. This in turn explains the 96 ± 1% densification of bimodal SiC samples at 1950°C (Figure 11a), which is at least 100°C lower than most literature reports for pressureless sintering. An important attribute of the higher solids loading in bimodal samples can be seen in Figure 11b where relatively lesser shrinkage (15% v/s 20-%) is needed to obtain 96 ± 1% densification, compared to prior reports.

A decrease in density is noticed after ~1950°C. This in turn can be correlated with the weight loss experienced by bimodal SiC samples during sintering as shown in the Figure 13. Such weight loss could be due to the formation volatile monoxides of Al and Y along with O_2.

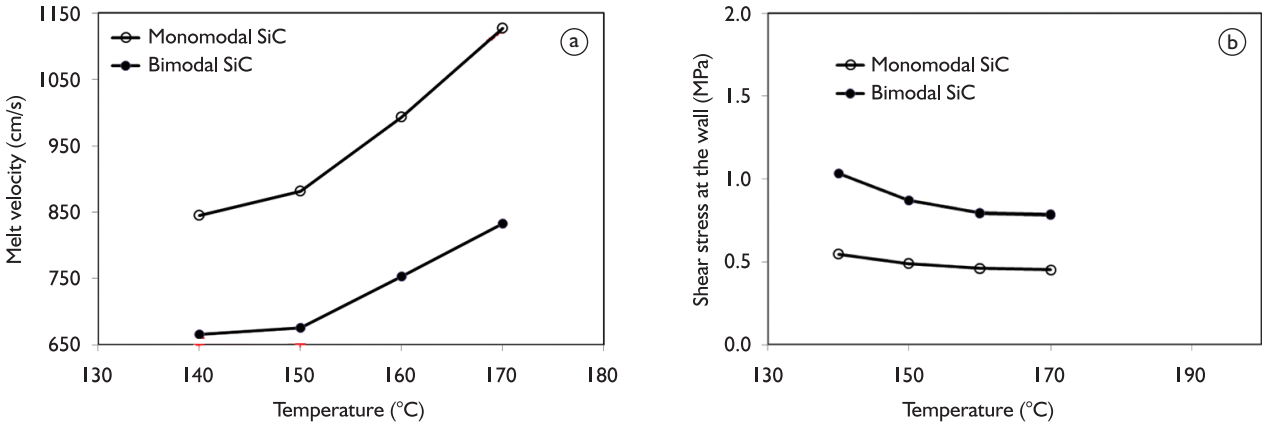

Figure 7. (a) Melt velocity and (b) shear stress at the wall as a function of injection temperature.

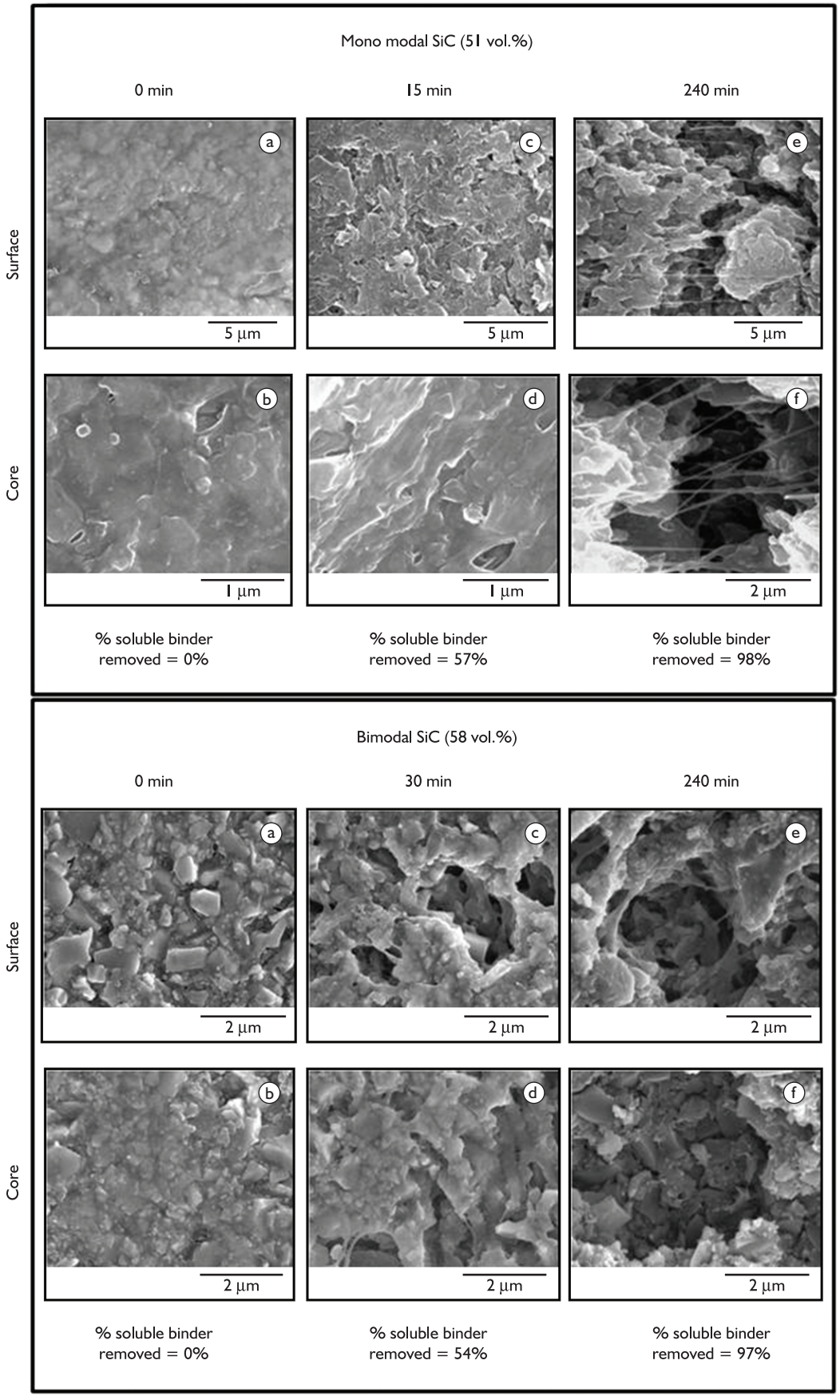

Figure 8. SEM of monomodal (left) and bimodal (right) SiC samples after various solvent debinding times.

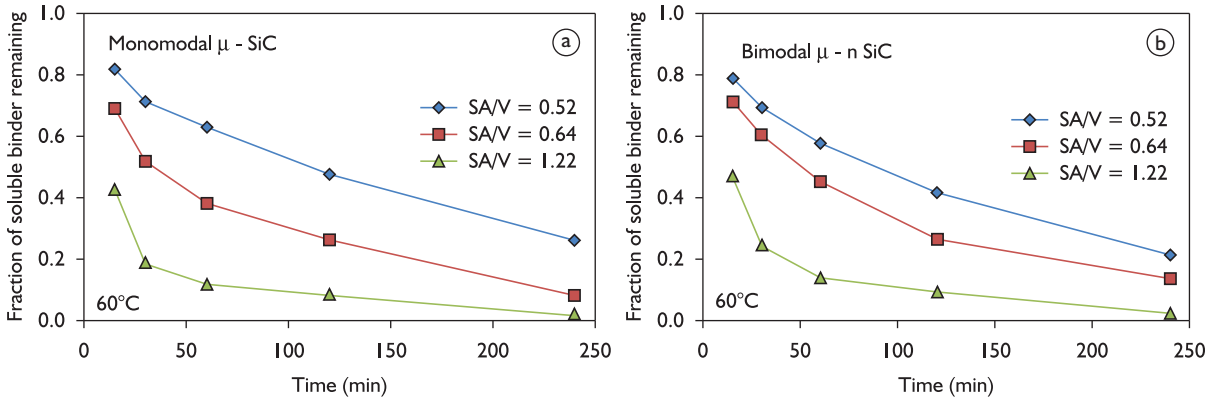

Figure 9. Solvent debinding kinetics of (a) monomodal and (b) bimodal SiC samples.

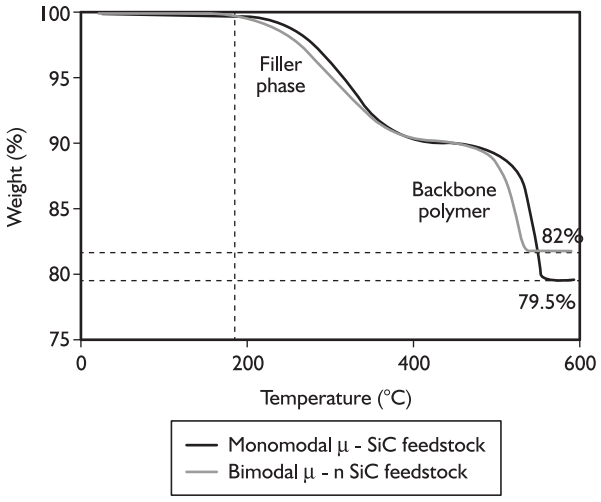

Figure 10. TGA of monomodal and bimodal SiC feedstocks.

This material loss is likely to open up new pores at sintering temperatures leading to reduction in the % density. Future experiments including TGA-assisted–mass spectroscopy and XRD analysis are required to explain the effect of nanoparticle addition on the weight loss in the bimodal SiC samples.

Despite the fact that monomodal and bimodal SiC samples reveal 96% densification, the higher amount of liquid phase additives, smaller grain size and higher weight loss could account for the lower thermal conductivity value of ~70 ± 2 W/m.K compared to that of previous reports (Figure 14a). In addition to thermal properties, the effect of sintering temperature on the mechanical properties of monomodal and bimodal SiC are studied (Figure 14b). A maximum Vickers hardness of 10.2 SGPa and indentation toughness of 2.3 MPa.m$^{1/2}$ is noticed for the SiC samples sintered at 1650°C. Similar values of

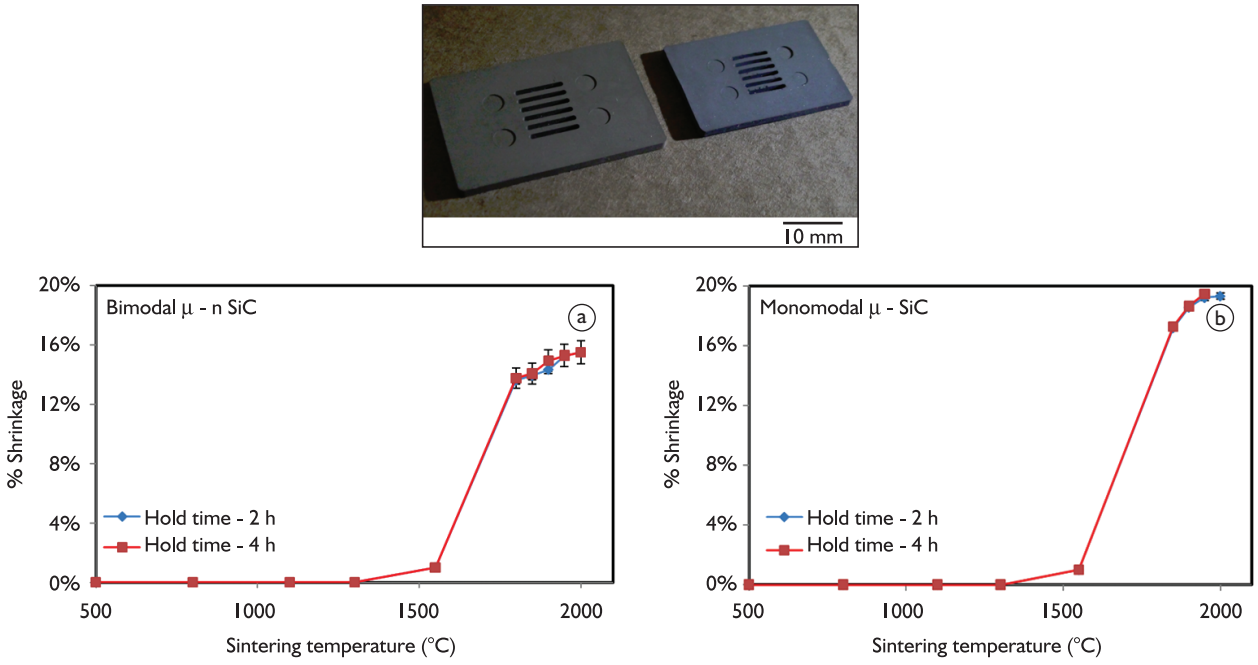

Figure 11. Shrinkage as a function of temperature for monomodal (right) and bimodal (left) SiC samples. Injection molded and sintered samples are shown for illustration (top).

hardness equivalent to 15 ± 0.2 GPa and an indentation toughness of 3.2 ± 0.1 MPa.m$^{1/2}$ have been reported in the past. Additionally, both the Vickers hardness and indentation toughness reduce with increase in temperatures, possibly due to porosity formation following weight loss. A detailed analysis with variations in the fabrication

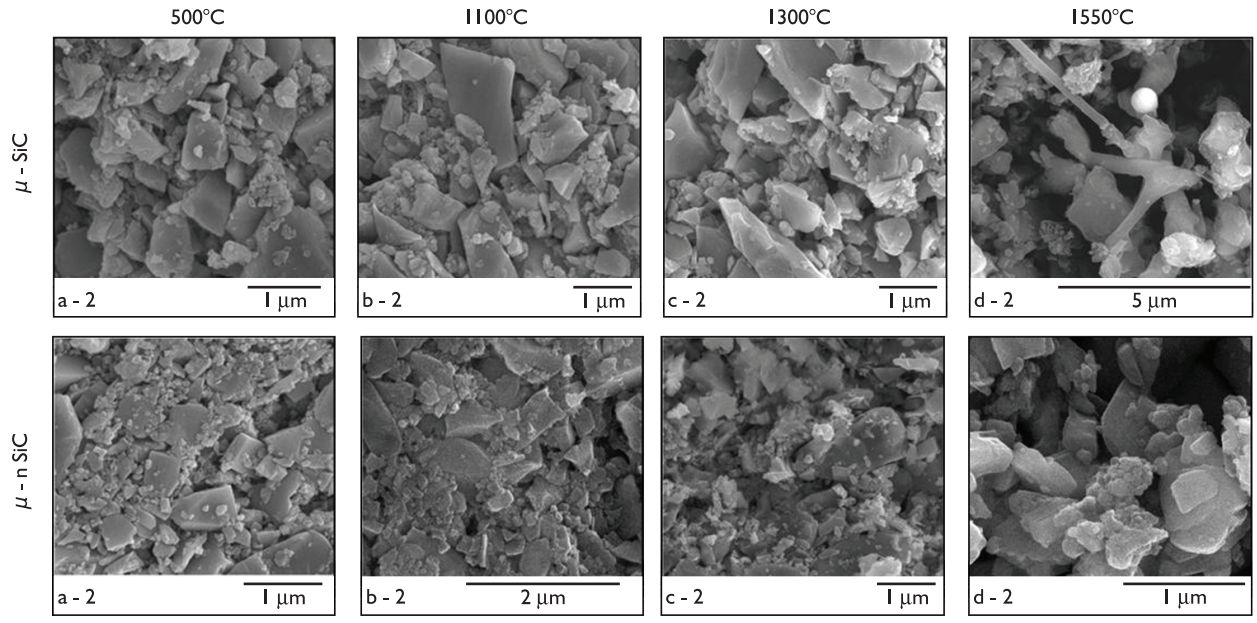

Figure 12. Differences in onset of sintering for monomodal (top) and bimodal (bottom) SiC samples, revealing a novel nanorod formation in the former system.

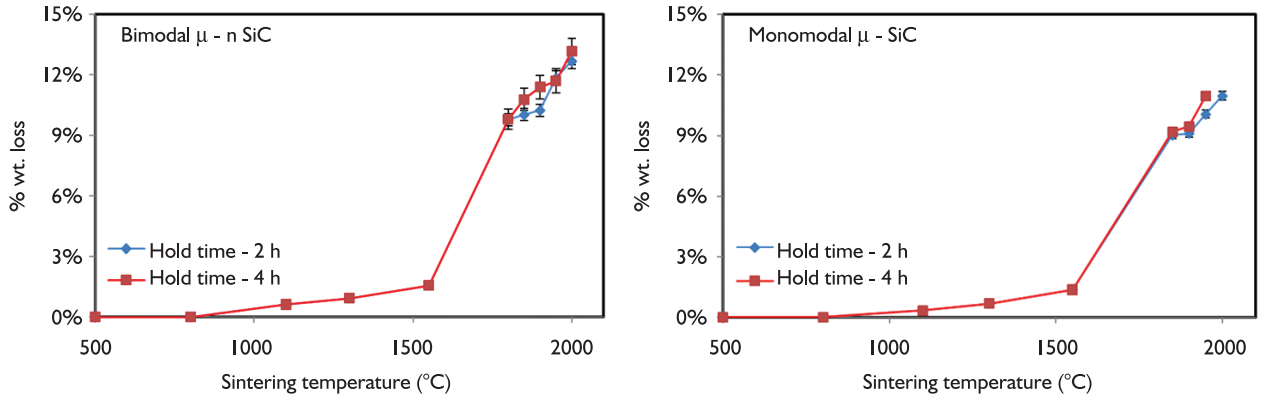

Figure 13. Weight loss during sintering of monomodal (right) and bimodal (left) SiC samples.

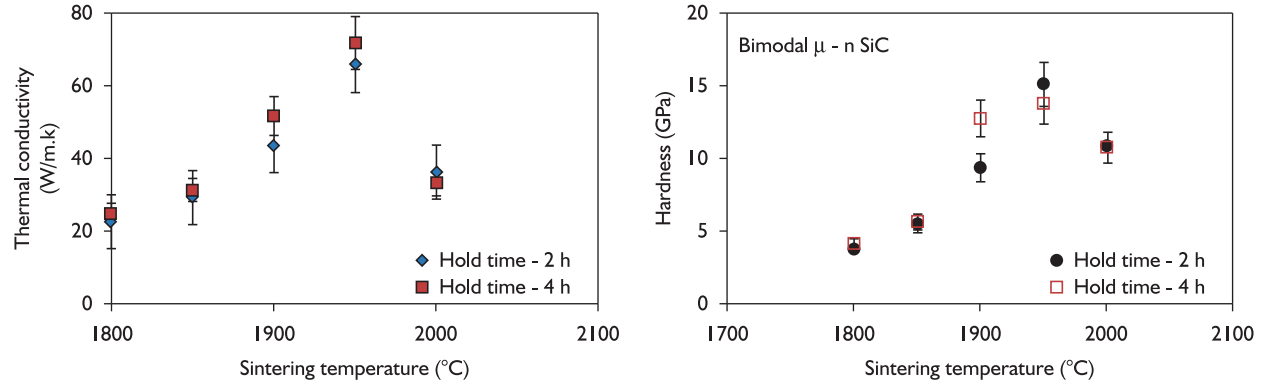

Figure 14. Thermal conductivity (left) and hardness (right) as a function of sintering temperature for bimodal SiC samples. Monomodal samples followed similar trends.

techniques and amount and composition of sintering aids is required to explore the possibility to improve the thermal and mechanical properties of bimodal SiC. Additionally, measurements on sintered monomodal μ-SiC samples are required to further study the effects of nanoparticle addition on the properties of SiC.

4 CONCLUSIONS

This paper presents an in-depth study on the effects of nanoparticle addition on the powder injection molding (PIM) of SiC powder-polymer mixtures. The following are some of the important conclusions obtained from this work:

- Bimodal mixtures of nanoscale and sub-micrometer particles are found to have significantly increased powder volume fraction (solids loading) in the mixtures for PIM;
- Rheological measurements conclude that at comparable solids loading, nanoparticle addition is found to reduce the viscosity of the resulting bimodal mixtures;
- Bimodal SiC samples exhibits slower polymer removal behavior compared to monomodal samples irrespective of the solvent debinding conditions;
- Bimodal SiC feedstocks exhibits enhanced polymer pyrolysis compared to monomodal samples during TGA, presumably due to catalytic effects, when the process is not diffusion controlled;
- Bimodal μ-n SiC samples exhibits a liquid phase formation at lower temperature of ~1550°C compared to that of the conventional monomodal μ- SiC samples with microscale additives that have been reported in the literature.
- Densification in bimodal samples appears to occur at a relative lower sintering temperature of ~1950°C, exhibiting >96% relative density. However, only 15% isometric shrinkage is observed for the bimodal system compared to 20% for the monomodal system; and
- A maximum Vickers hardness of 15 GPa and indentation toughness of 3.1 MPa.m$^{1/2}$ are measured for the monomodal and bimodal SiC samples sintered at 1950°C. Further sintering at higher temperatures reduces the mechanical and thermal properties.

REFERENCES

1 GERMAN, R. M.; BOSE, A. *Injection molding of metal and ceramics*. New Jersey: MPIF, 1997.

2 ONBATTUVELLI, V. P. et al. Properties of SiC and AlN feedstocks for the powder injection moulding of thermal management devices . *PIM International*, v. 4, n. 3, p. 64-70, Sep. 2010.

3 DABAK, T.; YUCEL, O. Shear viscosity behavior of highly concentrated suspensions at low and high shear-rates. *Rheologica Acta*, v. 25, n. 5, p. 527-33, Sep. 1986. http://dx.doi.org/10.1007/BF01774404

4 BAKAN, H. I. Injection moulding of alumina with partially water soluble binder system and solvent debinding kinetics. *Materials Science and Technology*, v. 23, n. 7, p. 787-91, July 2007. http://dx.doi.org/10.1179/174328407X161196

5 HWANG, K. S.; SHU, G. J.; LEE, H. J. Solvent debinding behavior of powder injection molded components prepared from powders with different particle sizes. *Metallurgical and Materials Transactions A*, v. 36, p.161-7, Jan. 2005. http://dx.doi.org/10.1007/s11661-005-0148-6

6 SURNEV, S.; LEPKOVA, D.; YOLEVA, A. Influence of the sintering additives on the phase composition and the thermal conductivity of aluminium nitride ceramics. *Materials Science and Engineering B*, v. 10, n. 3, p. 35-40, 1991. http://dx.doi.org/10.1016/0921-5107(91)90092-A

7 MOLISANI, A. L. et al. Effects of CaCO3 content on the densification of aluminum nitride. *Journal of the European Ceramic Society*, v. 26, n. 15, p. 3431-40, 2006. http://dx.doi.org/10.1016/j.jeurceramsoc.2005.08.010

8 GERMAN, R. M. *Sintering theory and practice*. New York: John Wiley and Sons, 1996.

9 ZHOU, H. et al. Effects of binary additives B2O3–Y2O3 on the microstructure and thermal conductivity of aluminum nitride ceramics. *Journal of Materials Science*, v. 34, n. 24, p. 6165-8, Dec. 1999. http://dx.doi.org/10.1023/A:1004782223271

10 LI, X. L. et al. AlN ceramics prepared by high-pressure sintering with La2O3 as a sintering aid. *Journal of Alloys and Compounds,* v. 463, n. 1-2, p. 412-6, Sep. 2008. http://dx.doi.org/10.1016/j.jallcom.2007.09.050

11 KUME, S. et al. Effects of annealing on dielectric loss and microstructure of aluminum nitride ceramics *Journal of American Ceramic Society*, v. 88, n. 11, p. 3229-31, Nov. 2005. http://dx.doi.org/10.1111/j.1551-2916.2005.00556.x

12 ONBATTUVELLI, V. P.; ATRE, S. V. Review of net shape fabrication of thermally conducting ceramics. *Materials and Manufacturing Processes*, v. 26, n.11, p. 832-45, 2011. http://dx.doi.org/10.1080/10426914.2010.515646

Recebido em: 05/11/2011
Aceito em: 02/03/2012